Kinetics Study of OH Radical Reactions with *n*-Octane, *n*-Nonane, and *n*-Decane at 240−340 K Using the Relative Rate/Discharge Flow/Mass Spectrometry Technique

Zhuangjie Li,* Sumitpal Singh, William Woodward, and Lan Dang

Department of Chemistry and Biochemistry, California State University Fullerton, Fullerton, California 92834

Received: June 19, 2006; In Final Form: September 1, 2006

The kinetics of the reactions of hydroxyl radical with *n*-octane (k_1), *n*-nonane (k_2), and *n*-decane (k_3) at 240−340 K and a total pressure of ∼1 Torr has been studied using relative rate combined with discharge flow and mass spectrometer (RR/DF/MS) technique. The rate constant for these reactions was found to be positively dependent on temperature, with an Arrhenius expression of $k_1 = (2.27 \pm 0.21) \times 10^{-11}\exp[(-296 \pm 27)/T]$, $k_2 = (4.35 \pm 0.49) \times 10^{-11}\exp[(-411 \pm 32)/T]$, and $k_3 = (2.26 \pm 0.28) \times 10^{-11}\exp[(-160 \pm 36)/T]$ cm^3 molecule^{-1} s^{-1} (uncertainties taken as 2σ), respectively. Our results are in good agreement with previous studies at and above room temperature using different techniques. Assuming that the reaction of alkane with hydroxyl radical is the predominant form for loss of these alkanes in the troposphere, the atmospheric lifetime for *n*-octane, *n*-nonane, and *n*-decane is estimated to be about 43, 35, and 28 h, respectively.

1. Introduction

Volatile organic compounds (VOCs) are organic molecules that consist of carbon chains or rings of varying sizes. Alkanes are a group of VOCs with only saturated C−C bonds and are used in many applications. For example, alkanes are often used as solvent blends in industry. High molecular weight *n*-alkanes, including *n*-octane, *n*-nonane, and *n*-decane, are important ingredients of gasoline and jet fuels.[1−3] Large amount of *n*-alkanes are anthropogenically emitted into the atmosphere because of evaporative emission as well as incomplete combustion of fuels.[2,4−6] The *n*-octane, *n*-nonane, and *n*-decane can also be emitted into the atmosphere through meat charbroiling.[7] As a result, the C_8-C_{10} *n*-alkanes are ubiquitously present in the atmosphere, and high mixing ratios of these *n*-alkanes at ppb level have been detected in the lower atmosphere in the United States as well as in other urban areas worldwide.[1,5−9] The C_8-C_{10} *n*-alkanes are found to contribute to air pollution. Air quality model studies have suggested that oxidation of 1.0 g of C_8-C_{10} *n*-alkane can lead to production of 0.46−1.11 g of ozone.[10,11] A more recent study also reported that *n*-alkanes with a chain of eight carbons or more can contribute to the formation of secondary organic aerosols.[12]

The *n*-alkanes are predominantly removed from the atmosphere by reacting with OH radicals during daytime.[4,13] The reaction of *n*-alkanes with OH radicals proceeds primarily with the abstraction of a H atom from the alkane molecule by the hydroxyl radical[4,13]

$$n\text{-}C_nH_{2n+2} + OH \rightarrow H_2O + n\text{-}C_nH_{2n+1}$$

In the presence of NO_x in the atmosphere, the resulting alkyl radical, n-C_nH_{2n+1}, will further degrade leading to formation of tropospheric ozone and alkyl nitrates.[4,13−15] Since the reaction with OH radicals initiates the oxidative degradation of the VOCs, it is important to acquire kinetic information about the interaction between the OH radicals and *n*-alkanes to understand the photochemical smog system. Numerous experimental kinetic studies had been carried out for the reactions of OH radicals with C_8-C_{10} *n*-alkanes using various techniques, including shock tube,[16] high-pressure discharge flow combined with laser-induced fluorescence,[17] flash photolysis,[18] static relative rate,[19−26] and flow relative rate[27] techniques. However, previous investigations of OH reaction with C_8-C_{10} *n*-alkanes have primarily been limited to temperatures equal to or higher than room temperature, and there have been very few experimental examinations for these reactions at temperatures mimicking the atmospheric conditions except a most recent study reported by Wilson et al.[26] To facilitate better modeling the atmospheric chemistry of VOCs, it is necessary to acquire kinetic parameters of the reactions of OH with VOCs at temperatures representative of troposphere. Our laboratory is therefore conducting a series of kinetic investigations for the reactions of VOCs with atmospheric oxidants, such as OH and Cl, at a temperature range imitating the troposphere using the relative rate/discharge flow/mass spectrometer technique (RR/DF/MS) that was recently developed in our laboratory.[27] One important goal of our investigations is to expand the existing kinetic database for the reactions of OH with VOCs to tropospheric temperature region, which is needed to predict the atmospheric lifetime of these compounds and to better model their atmospheric chemistry. In this paper, we report the rate constants for the reactions of OH radical with *n*-octane (k_1), *n*-nonane (k_2), and *n*-decane (k_3) at 240−340 K

$$n\text{-}C_8H_{18} + OH \rightarrow H_2O + n\text{-}C_8H_{17} \quad (1)$$

$$n\text{-}C_9H_{20} + OH \rightarrow H_2O + n\text{-}C_9H_{19} \quad (2)$$

$$n\text{-}C_{10}H_{22} + OH \rightarrow H_2O + n\text{-}C_{10}H_{21} \quad (3)$$

We will also comment on the atmospheric lifetime of those compounds on the basis of our experimental results.

2. Experimental Section

The RR/DF/MS technique has previously been employed in kinetics investigation of VOCs reaction with OH and Cl radicals

* Author to whom correspondence should be addressed. Phone: (714)-278-3585. Fax: (714)626-8010. E-mail: zli@fullerton.edu.

10.1021/jp0638134 CCC: $33.50
Published on Web 10/18/2006

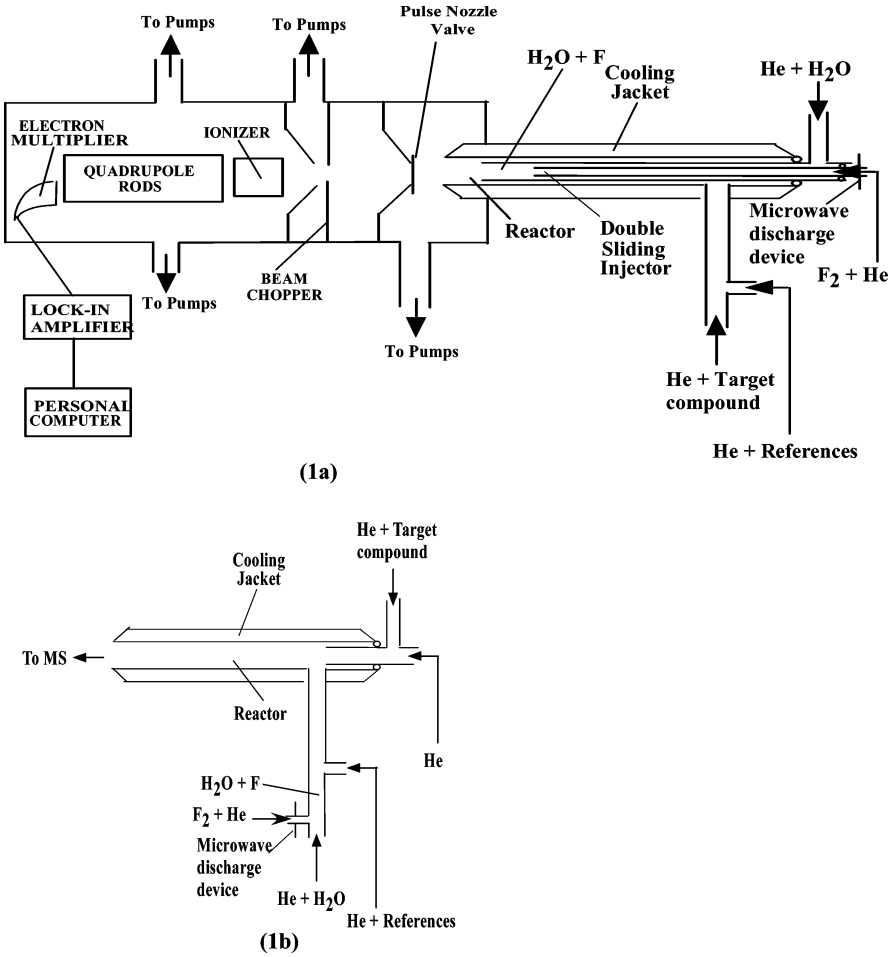

Figure 1. Experimental apparatus for RR/DF/MS study of *n*-alkanes + OH radical reaction at 240−320 K (1a) and for the controlled experiments (1b). For all kinetic experiments, F atom is produced by microwave discharge of F_2 in the sliding injector. H_2O is added through the outer sliding injector as the OH precursor. Both *n*-alkane and reference compounds are mixed and introduced into the reactor from sidearm.

at 240−340 K.[28,29] Figure 1 shows experimental apparatus used in the RR/DF/MS study of *n*-alkanes reaction with OH radicals. The RR/DF/MS system has been described previously[27] and is only briefly discussed here. The flow reactor is made of a Pyrex tube (length: 80 cm, i.d.: 5.08 cm). The internal surface of the reactor is covered with a layer of poly(tetrafluoroethylene) (TFE) Teflon sheet (0.05-cm thick) to reduce the OH radical wall loss. A steady-state gas flow in the flow tube is achieved by using a mechanical pump (Edwards E2M175). The vacuum chamber housing the mass spectrometer is a two-stage differentially pumped vacuum system utilizing two 6-in. diffusion pumps with liquid nitrogen baffles, and the ultimate vacuum in the second stage is $<5 \times 10^{-10}$ Torr. Helium is used as a carrier gas and is introduced into the flow reactor through both a double-sliding injector and a sidearm inlet port located upstream of the reactor. A total pressure of about 1 Torr in the flow reactor is maintained through continuous pumping during the experiments. Mean gas velocity in the flow tube is about 1200 cm s^{-1}. With an injector moving distance of 30 cm, the corresponding gaseous residence times in the reactor are about 24 ms. A removable liquid nitrogen trap is placed downstream of the reactor to protect the mechanical pump from corrosive reactants and products.

Mass spectrometric detection of reactants and products is carried out by continuous sampling at the downstream end of the flow tube through a two-stage beam inlet system. The mass spectrometer (Extrel Model MAX-1000) is set to emit bombarding electrons with 40 eV of impact energy for ionization of chemicals in the flow reactor. Beam modulation is accomplished with a 200 Hz tuning fork chopper (Electrooptical Products Corp. CH-10) placed inside the second stage of the inlets. Ion signals are sent to a lock-in amplifier (Stanford Research Systems SR510) that was referenced to the chopper frequency. The amplified analog signals are then converted to digital form (Analog Devices RTI/815) and are recorded on a microcomputer. Under normal operating conditions, the detection limit for the mass spectrometer is about 10^9-10^{10} molecules cm^{-3}, depending on the individual species detected.

The OH radicals are produced by reacting F atoms with H_2O in a double-sliding injector

$$F + H_2O \rightarrow OH + HF \qquad k_4 = 1.4 \times 10^{-11}\ cm^3\ molecule^{-1}\ s^{-1}\ ^{130} \quad (4)$$

The double-sliding injector consisted of two concentric Pyrex tubes with internal diameters of 7 mm and 12.7 mm. The H_2O vapor is carried by 100 sccm of helium to the double-sliding injector to react with the fluorine atoms generated by microwave discharge (OPTHOS INSTRUMENTS, INC. Model MPG-4) of 5% F_2 that is carried by 1500 sccm of helium. The discharge of F_2 is taking place in a ceramic tube within the microwave discharge cavity. The internal surface of inner Pyrex tube is coated with halocarbon wax (series 1500, Halocarbon Products Corp.) to reduce F atom loss because of reaction with SiO_2.

Both target (either *n*-octane or *n*-nonane or *n*-decane) and reference compounds (either 1,4-dioxane or diethyl ether) are

carried by 100∼200 sccm of helium and are introduced into the flow reactor from a sidearm inlet port. Prior to entering the reactor, the target and reference compounds are mixed to ensure that they share the same reaction time with the OH radicals inside the reactor.

The reactor temperatures are varied and controlled at 240−340 K using a temperature bath circulator (Neslab ULT-80) by circulating either methanol or water through an outer Pyrex jacket for experiments either at low (T < 298 K) or at high (T ≥ 298 K) temperatures, respectively. Each temperature-dependent experiment is performed two to four times at different days under the same experimental conditions to check the consistency of the experimental results.

On the basis of the theory of the RR/DF/MS technique,[27] rate constant determination for the hydroxyl radical reaction with a target alkane compound is briefly described as the following:

$$\text{alkane} + \text{OH} \rightarrow \text{products} \quad (5)$$

$$\text{reference compound} + \text{OH} \rightarrow \text{products} \quad (6)$$

Assuming that the alkane and reference compounds react only with OH radicals, then it has been shown[27] that

$$\ln \frac{[\text{alkane}]_{t,0}}{[\text{alkane}]_{t,[\text{OH}]}} = \frac{k_{\text{alkane+OH}}}{k_{\text{reference+OH}}} \ln \frac{[\text{reference}]_{t,0}}{[\text{reference}]_{t,[\text{OH}]}} \quad \text{(I)}$$

where $[\text{alkane}]_{t,0}$ and $[\text{reference}]_{t,0}$ are the concentrations of the alkane and the reference compounds in the absence of OH radicals at time t, $[\text{alkane}]_{t,[\text{OH}]}$ and $[\text{reference}]_{t,[\text{OH}]}$ are the concentrations of the alkane and the reference compound in the presence of OH radicals at time t, and $k_{\text{alkane+OH}}$ and $k_{\text{reference+OH}}$ are the rate constants for reactions 5 and 6, respectively. By monitoring the decay of both the alkane and the reference compounds, a straight line with a slope equal to $k_{\text{alkane+OH}}/k_{\text{reference+OH}}$ is expected to be generated from the plot of $\ln([\text{alkane}]_{t,0}/[\text{alkane}]_{t,[\text{OH}]})$ versus $\ln([\text{reference}]_{t,0}/[\text{reference}]_{t,[\text{OH}]})$. The $k_{\text{alkane+OH}}$ can then be calculated if the absolute of $k_{\text{reference+OH}}$ is known. Also, if the temperature dependence of $k_{\text{reference+OH}}$ is known, repeating the above exercise at different temperatures allows determination of the temperature dependence for $k_{\text{alkane+OH}}$. In the present work, experiments are carried out at a temperature range of 240−340 K.

The concentration of the species in the flow reactor is determined either by flowing the known amount of sample into the reactor or by quantitative conversion of the species through chemical reactions. In particular, the initial concentration of the OH radicals is taken to be the same as the atomic fluorine concentration, which is determined by measuring the $[F_2]$ difference between "switch on" and "switch off" of the microwave discharge device while F_2 is passing through the discharge cavity:[29] $[F] = 2\Delta[F_2] = 2([F_2]_{\text{switch off}} - [F_2]_{\text{switch on}})$. It is found that 90−98% of the F_2 dissociates under 50 W of microwave discharge power, with dissociation efficiency inversely proportional to the amount of F_2. Excessive amount of water (∼7×10^{14} molecule cm^{-3}) is introduced into the double-sliding injector to ensure complete titration of the fluorine atoms in the present work, and thus the variation of the OH radical concentration is achieved by altering the amount of F_2 ($(0-5) \times 10^{13}$ molecule cm^{-3}) passing through the cavity.

During the experiments, *n*-octane, *n*-nonane, *n*-decane, 1,4-dioxane, and diethyl ether are monitored by the mass spectroscopic detection of their parent ion at m/z = 114, 128, 142, 88, and 74, respectively. It is found that under our experimental conditions no significant fragment daughter ions at m/z = 88 or 74 are generated either from the C_8-C_{10} *n*-alkanes or from the C_8-C_{10} *n*-alkyl radical products. Therefore, there is essentially very little interference in our mass spectroscopic detection of all parent ions, and the decay of these reactants after introducing OH into the flow reactor is considered to be primarily due to reaction of these reactants with the OH radicals.

Helium (>99.99%) is obtained from Oxygen Service Company. F_2 (5% balanced in He) is obtained from Spectra Gases, Inc. The following reactants are purchased from Fisher Scientific Company: *n*-decane, >99%; 1,4-dioxane, >99%. The *n*-octane, with a purity of >99%, is purchased from Aldrich Chemical Co., Inc. The *n*-nonane, with a purity of >99%, is purchased from Chevron Phillips Chemical Company. The diethyl ether with a purity of >99% is obtained from EMD chemicals Inc. All samples are used as received. Distilled water is used as the OH precursor.

3. Results and Discussion

Kinetic data for reactions 1−3 were acquired with the RR/DF/MS technique. The experimental data were collected at 298 K and a total pressure of 1−1.1 Torr using 1,4-dioxane and diethyl ether as reference compounds to check the consistency of the kinetics results. Temperature-dependent kinetics study was conducted at 240−340 K using 1,4-dioxane as reference compound.

To ensure high-quality kinetics results, control experiments and model simulation were carried out in the present work to address the concerns regarding the potential effects on the decay of both target and reference compounds because of secondary reactions involved in our chemical system. The control experiments were designed to examine if the primary products, that is, the alkyl radicals *n*-C_xH_{2x+1} (x = 8−10), from reactions 1−3 further reacted with the reference compounds that would contribute to the decay of the reference compounds. The control experiments were also used to examine if the primary products, that is, the $C_4H_7O_2$ and CH_3OCH_2 radicals, from reaction 6 further reacted with *n*-octane, *n*-nonane, and *n*-decane to affect the decay of the *n*-alkanes. The experimental setup for the control experiments is shown in Figure 1b, in which the OH radicals produced from the sidearm of the reactor reacted with a reference compound (or a target compound) while traveling through the sidearm.[29] The primary products then entered the reactor to interact with an *n*-alkane compound (or a reference compound). This arrangement allows monitoring of the effects on the decay of the reference compound (or target compound) because of the direct contacts between the *n*-C_xH_{2x+1} (x = 8−10) radicals and the reference compounds or between the $C_4H_7O_2$ and CH_3OCH_2 radicals and *n*-alkane molecules. It was found that the products from OH + 1,4-dioxane or diethyl ether had little effect on the *n*-alkane mass spectral signal intensity (<1%). Likewise, the products from the OH + *n*-alkane reaction had little effect on the 1,4-dioxane or diethyl ether mass spectral intensity (<3.5%). This indicates that the decay of both target and reference compounds is not significantly affected by the primary products of the reactions of OH + reference compound and OH + target compound, respectively.

Model simulation calculations were also performed to investigate the potential effects of the atomic oxygen and atomic hydrogen produced from the secondary reaction in our chemical

system on the decay of the target and reference compounds via

$$OH + OH \rightarrow H_2O + O$$
$$k_7 = 1.9 \times 10^{-12}\ cm^3\ molecule^{-1}\ s^{-1}\ ^{30} \quad (7)$$

$$O + OH \rightarrow O_2 + H$$
$$k_8 = 3.3 \times 10^{-11}\ cm^3\ molecule^{-1}\ s^{-1}\ ^{30} \quad (8)$$

$$O + \text{target compound} \rightarrow OH + \text{other products} \quad (9)$$

$$O + \text{reference compound} \rightarrow OH + \text{other products} \quad (10)$$

$$H + \text{target compound} \rightarrow H_2 + \text{other products} \quad (11)$$

$$H + \text{reference compound} \rightarrow H_2 + \text{other products} \quad (12)$$

The model used the fourth-order Runge−Kutta method to numerically solve differential equations specifying a chemical system and calculated the concentration of chemical species of interest in the chemical system as a function of time.[31] Using a chemical system and rate parameters adapted from Li[27] including reactions 5−12 with initial concentrations of (1.3−1.6) × 10^{14} molecule cm^3 and (5.9−6.5) × 10^{13} molecule cm^3 for the *n*-alkanes and reference compounds and an initial concentration of about 9.0 × 10^{13} molecule cm^3 for the OH radical, respectively, our simulation calculation results predicted that in 30 ms of reaction time in the flow tube more than 99.9% of the OH radicals are removed and less than 1% of the target and reference compounds can be consumed by reactions 9−12. This indicates that the atomic oxygen and atomic hydrogen have very little effect on the decay of target and reference compounds, and the kinetics data acquired under our experimental conditions were essentially free from the interference of secondary reactions.

A. OH + *n*-Octane. Figure 2 shows the kinetic data for the reaction of *n*-octane with OH radicals at 298 K using 1,4-dioxane (Figure 2a) and diethyl ether (Figure 2b) as reference compounds. The decay of both *n*-octane and reference compounds can be portrayed by eq I. A linear regression of the experimental data produced a rate constant ratio of $k_1/k_{6,1,4-\text{dioxane}}$ = 0.778 ± 0.026 and $k_1/k_{6,\text{diethyl ether}}$ = 0.737 ± 0.052, respectively. The recommended rate constant for the reaction of hydroxyl radical with 1,4-dioxane and diethyl ether was $k_{6,1,4-\text{dioxane}}$ = (1.09 ± 0.07) × 10^{-11} and $k_{6,\text{diethyl ether}}$ = (1.30 ± 0.06) × 10^{-11} cm^3 $molecule^{-1}$ s^{-1}, respectively.[32,33] The rate constant for reaction 1 was then determined to be k_1 = (8.48 ± 0.61) × 10^{-12} and k_1 = (9.58 ± 0.80) × 10^{-12} cm^3 $molecule^{-1}$ s^{-1} at 298 K using 1,4-dioxane and diethyl ether as the reference compounds, respectively. The quoted error bars were taken as 2σ for this work, which have taken into account the scatter of data and uncertainty of the experimental parameters such as pressure, temperature, flow rates, and the uncertainty of the reference rate constant. Within the experimental uncertainty, the rate constant is in very good agreement with the previous value of (8.88 ± 0.31) × 10^{-12} cm^3 $molecule^{-1}$ s^{-1} reported by Li using 1,4-dioxane as the reference, indicating a good reproducibility and consistency of the RR/DF/MS technique. The rate constant values obtained using two different references differ by about 10%. An average of k_1 = (9.03 ± 0.80) × 10^{-12} cm^3 $molecule^{-1}$ s^{-1} is derived for the reaction of OH with *n*-octane at 298 K, which is also in good agreement with most previous investigations for this reaction[18,22,23,27] as summarized in Table 1. However, our k_1 value at 298 K is higher than the most recent value of 7.43 × 10^{-12} cm^3 $molecule^{-1}$ s^{-1} reported by Wilson et al.[26] Part of this discrepancy could be attributed to the value of the reference rate constants of OH + *n*-heptane and OH + cyclohexane used in deriving the k_1 value in Wilson et al.'s work, which are smaller than the recommended values by 4−6%.[34]

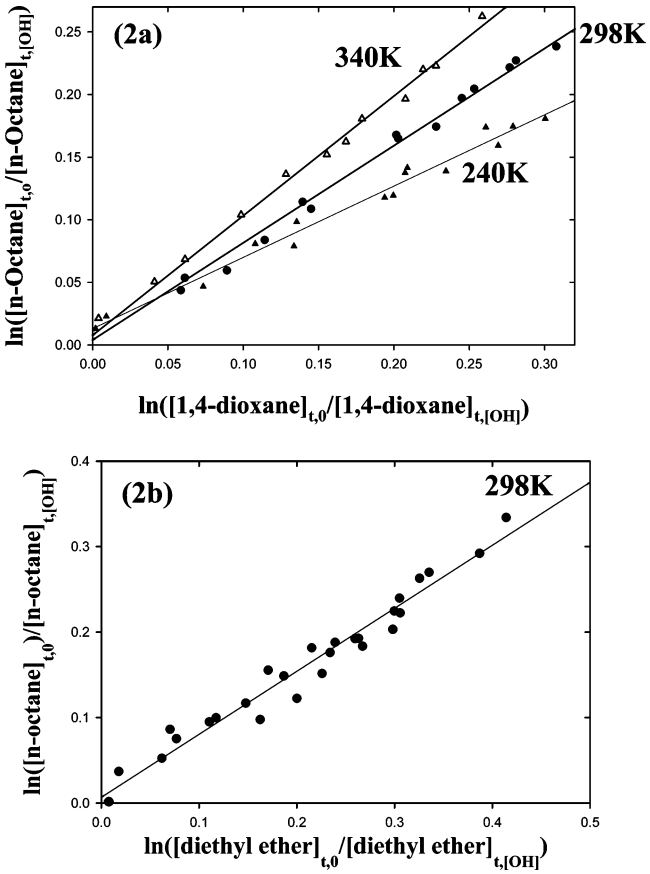

Figure 2. Typical kinetic data acquired with the RR/DF/MS technique at 240−340 K and a fixed reaction time of 24 ms for the reaction of *n*-octane with OH radical using 1,4-dioxane (2a) and diethyl ether (2b) as reference. The experiments are carried out at a total pressure of 1.0−1.1 Torr. Initial concentrations are (1.71−3.84) × 10^{14}, (3.97−7.57) × 10^{13}, and (0.84−1.65) × 10^{14} molecules cm^{-3} for *n*-octane, 1,4-dioxane, and diethyl ether, respectively. The OH concentration is varied in a range of (0−9.4) × 10^{13} molecules cm^{-3}.

The rate constant of reaction 1 was also determined at 240, 260, 277, 320, and 340 K using 1,4-dioxane as a reference compound, and the results are shown in Figure 2a and are also listed in Table 1. Figure 3 shows the Arrhenius plot for reaction 1. An Arrhenius expression was then derived from the plot to be k_1 = (2.27 ± 0.21) × 10^{-11} exp[−(296 ± 27)/T] cm^3 $molecule^{-1}$ s^{-1} at 240−340 K. This result is in good agreement with the Arrhenius expression of k_1 = 2.57 × 10^{-11} × exp[−(332 ± 65)/T] cm^3 $molecule^{-1}$ s^{-1} reported by Greiner[18] at 296−497 K but is in contrast to the expression of k_1 = (4.52 ± 0.37) × 10^{-11} exp[−(538 ± 27)/T] cm^3 $molecule^{-1}$ s^{-1} at 284−384 K reported by Wilson et al.[26] Further investigations are needed to resolve the difference between these studies.

B. OH + *n*-Nonane. Figure 4 shows kinetic data of reaction 2 at 298 K using 1,4-dioxane (Figure 4a) and diethyl ether (Figure 4b) as reference compounds. Both sets of data can also be well described by eq I and a linear regression of the data in Figure 4 produced a rate constant ratio of $k_2/k_{6,1,4-\text{dioxane}}$ = 1.035 ± 0.092 and $k_2/k_{6,\text{diethyl ether}}$ = 0.870 ± 0.052, respectively. The rate constant for reaction 2 is then determined to be k_2 = (1.13 ± 0.12) × 10^{-11} and k_2 = (1.13 ± 0.09) × 10^{-11} cm^3 $molecule^{-1}$ s^{-1} at 298 K using 1,4-dioxane and diethyl ether as

TABLE 1: Rate Constant for OH + *n*-Octane at 240−340 K

T (K)	reference compound[a]	slope[b]	$k_1 \times 10^{12}$ (cm^3 molecule^{-1} s^{-1})	P_{total} (Torr)	technique[c]	reference
240	1,4-dioxane	0.577 ± 0.028 (23)	6.69 ± 0.56	1.0−1.1	RR/DF/MS	this work
260	1,4-dioxane	0.630 ± 0.018 (31)	7.12 ± 0.54	1.0−1.1	RR/DF/MS	this work
277	1,4-dioxane	0.713 ± 0.020 (30)	7.91 ± 0.55	1.0−1.1	RR/DF/MS	this work
298	1,4-dioxane	0.778 ± 0.026 (32)	8.48 ± 0.61	1.0−1.1	RR/DF/MS	this work
320	1,4-dioxane	0.809 ± 0.022 (35)	8.66 ± 0.61	1.0−1.1	RR/DF/MS	this work
340	1,4-dioxane	0.926 ± 0.032 (58)	9.73 ± 0.73	1.0−1.1	RR/DF/MS	this work
298	diethyl ether	0.737 ± 0.052 (29)	9.58 ± 0.80	1.0−1.1	RR/DF/MS	this work
296	n/a	n/a	8.42 ± 1.25	97.50	AR/FP/GC	[18]
298	1,4-dioxane	0.800 ± 0.028	8.88 ± 0.31	1.0−1.1	RR/DF/MS	[27]
299 ± 2	*n*-hexane	n/a	9.02 ± 0.11	735	RR/DP/GC	[23]
312	*n*-heptane	n/a	8.79 ± 0.31	757.5	RR/DP/GC	[22]
320	n/a	n/a	9.10	97.50	AR/FP/GC	[18]
340	n/a	n/a	9.68	97.50	AR/FP/GC	[18]
298	*n*-heptane/cyclohexane	1.173/1.092	7.43	760	GC/MS	[26]

[a] The rate constants of the hydroxyl radical reaction with 1,4-dioxane and diethyl ether were calculated from Arrhenious equations previously published.[32,33] [b] The error bar was taken as 2σ. The number in parentheses represents the number of data points collected at corresponding temperature. [c] AR, absolute rate; RF, relative rate; DF, diffraction flow; DP, direct photolysis; MS, mass spectrometer; FP, flash photolysis; GC, gas chromatography; FID, flame ionization detection; P, photolysis.

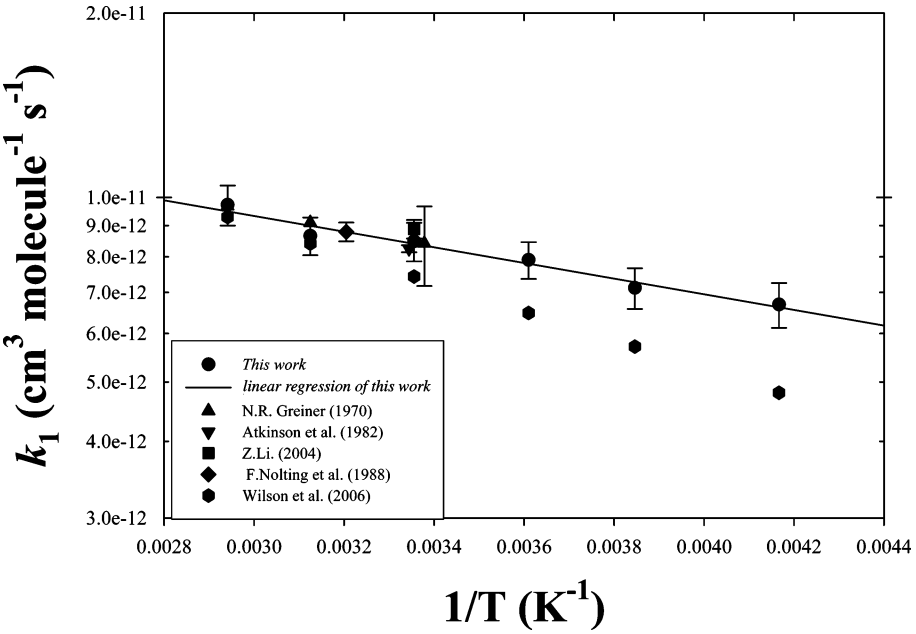

Figure 3. Arrhenius plot for the reaction of *n*-octane + OH at 240−340 K.

TABLE 2: Rate Constant for OH + *n*-Nonane at 240−340 K

T (K)	reference compound[a]	slope[b]	$k_2 \times 10^{11}$ (cm^3 molecule^{-1} s^{-1})	P_{total} (Torr)	technique[c]	reference
240	1,4-dioxane	0.692 ± 0.044 (44)	0.803 ± 0.075	1.0−1.1	RR/DF/MS	this work
260	1,4-dioxane	0.776 ± 0.068 (41)	0.877 ± 0.098	1.0−1.1	RR/DF/MS	this work
277	1,4-dioxane	0.873 ± 0.068 (31)	0.969 ± 0.097	1.0−1.1	RR/DF/MS	this work
298	1,4-dioxane	1.035 ± 0.092 (51)	1.13 ± 0.12	1.0−1.1	RR/DF/MS	this work
320	1,4-dioxane	1.083 ± 0.104 (30)	1.16 ± 0.14	1.0−1.1	RR/DF/MS	this work
340	1,4-dioxane	1.268 ± 0.128 (34)	1.33 ± 0.16	1.0−1.1	RR/DF/MS	this work
298	diethyl ether	0.870 ± 0.052 (35)	1.13 ± 0.09	1.0−1.1	RR/DF/MS	this work
299 ± 2	*n*-hexane	n/a	1.07 ± 0.04	735	RR/DP/GC	[23]
312	*n*-heptane	n/a	1.02 ± 0.03	758	RR/DP/GC	[22]
300	*n*-octane	n/a	1.03 ± 0.02	n/a	RR	[34]
296 ± 2	propene	n/a	1.02 ± 0.26	760	RR/P/GC-FID	[35]
295 ± 2	*n*-octane	n/a	0.99 ± 0.30	760	RR/P/GC-FID	[24]
295 ± 2	*n*-octane	n/a	1.016 ± 0.023	750	RR/FP/RF	[25]
294 ± 2	*n*-octane	n/a	0.95 ± 0.02	760	RR/ASC	[36]

[a] The rate constants of the hydroxyl radical reaction with 1,4-dioxane and diethyl ether were calculated from Arrhenious equations previously published.[32,33] [b] The error bar was taken as 2σ. The number in parentheses represents the number of data points collected at corresponding temperature. [c] RF, relative rate; DF, diffraction flow; DP, direct photolysis; MS, mass spectrometer; FP, flash photolysis; GC, gas chromatography; FID, flame ionization detection; P, photolysis.

the reference compounds, respectively. The two rate constant values determined using different reference compounds are in excellent agreement with each other, confirming that the RR/DF/MS technique produces consistent kinetic results. The average of two values yields $k_2 = (1.13 \pm 0.12) \times 10^{-11}$ cm^3 molecule^{-1} s^{-1} for the reaction of *n*-nonane with OH at 298 K.

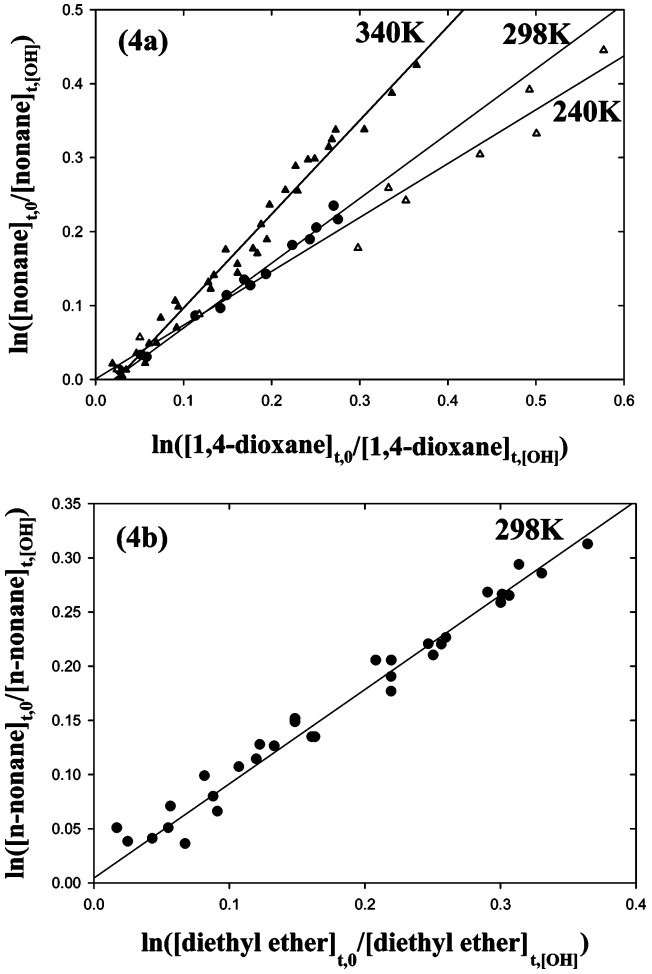

Figure 4. Typical kinetic data acquired with the RR/DF/MS technique at 240−340 K and a fixed reaction time of 24 ms for reaction of *n*-nonane with OH radical using 1,4-dioxane (4a) and diethyl ether (4b) as reference compounds. The experiments are carried out at a total pressure of 1.0−1.1 Torr. Initial concentrations of *n*-nonane, 1,4-dioxane, and diethyl ether are (2.07−4.15) × 10^{14}, (3.97−7.57) × 10^{13}, and (0.84−1.65) × 10^{14} molecules cm^{-3}, respectively. The OH concentration is varied in a range of (0−9.4) × 10^{13} molecules cm^{-3}.

Table 2 shows our kinetic parameters for the reaction of OH + *n*-nonane along with available values of k_2 in the literature for comparison. Previously reported k_2 values are in the range of (0.95−1.07) × 10^{-11} cm^3 $molecule^{-1}$ s^{-1}.[22−25,34−36] Our k_2 values are slightly higher than these values but are still in very good agreement with these studies within the experimental uncertainty.

The rate constant for the reaction of OH with *n*-nonane was also measured at 240, 260, 277, 320, and 340 K in the present work using 1,4-dioxane as reference compound. Figure 5 shows the Arrhenius plot of reaction 2, which leads to an Arrhenius equation of $k_2 = (4.35 \pm 0.49) \times 10^{-11} \exp[-(411 \pm 32)/T]$ cm^3 $molecule^{-1}$ s^{-1} at 240−298 K for this reaction. To the best of our knowledge, this is the first temperature-dependent kinetics study of reaction 2.

C. OH + *n*-Decane. Figure 6 shows the typical kinetic data for the reaction of OH with *n*-decane using 1,4-dioxane (Figure 6a) and diethyl ether (Figure 6b) as reference compounds at 298 K. Linear regression for the data in the plots produced a rate constant ratio of k_3/k_6 (1,4-dioxane as reference) = 1.183 ± 0.065 and k_3/k_6 (diethyl ether as reference) = 1.072 ± 0.038, respectively. The k_3/k_6 value obtained using 1,4-dioxane as the reference compound is in excellent agreement with the value

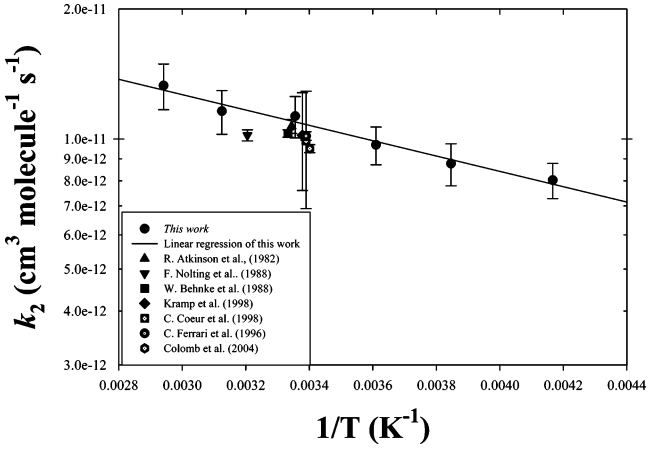

Figure 5. Arrhenius plot for the reaction of *n*-nonane + OH at 240−340 K.

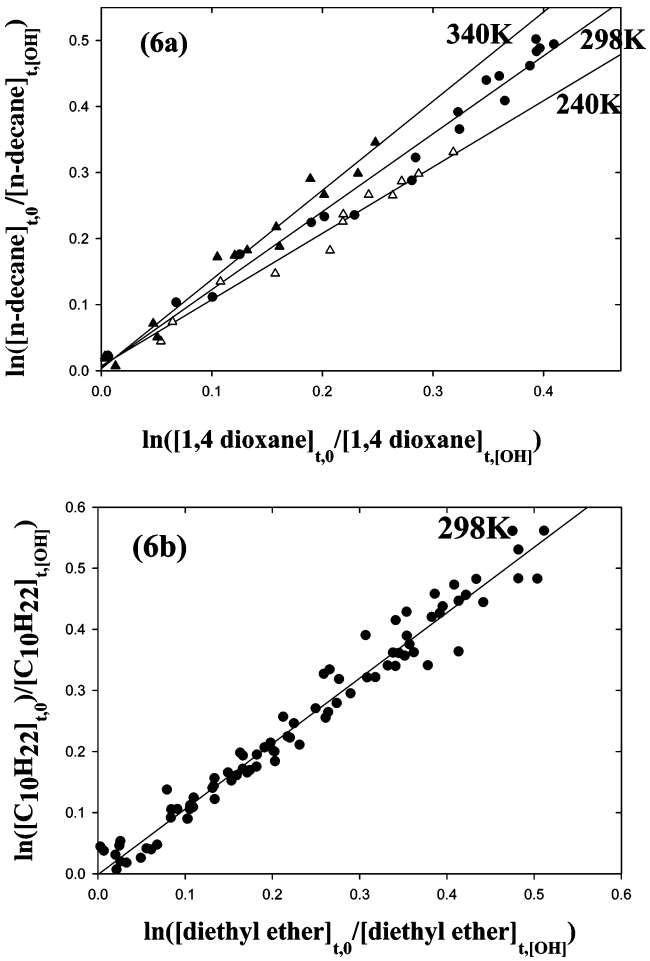

Figure 6. Typical kinetic data acquired with the RR/DF/MS technique at 240−340 K and a fixed reaction time of 24 ms for reaction of *n*-decane with OH radical using 1,4-dioxane (6a) and diethyl ether (6b) as reference compounds. The experiments are carried out at a total pressure of 1.0−1.1 Torr. Initial concentrations of *n*-decane, 1,4-dioxane, and diethyl ether are (1.53−4.13) × 10^{14}, (3.97−7.57) × 10^{13}, and (0.84−1.65) × 10^{14} molecules cm^{-3}, respectively. The OH concentration was varied in a range of (0−9.4) × 10^{13} molecules cm^{-3}.

previously reported by Li.[27] The rate constant for reaction 3 was then determined to be $k_3 = (1.29 \pm 0.11) \times 10^{-11}$ and $k_3 = (1.39 \pm 0.08) \times 10^{-11}$ cm^3 $molecule^{-1}$ s^{-1} at 298 K with 1,4-dioxane and diethyl ether as references, respectively. The average of these values yields $k_3 = (1.34 \pm 0.11) \times 10^{-11}$ cm^3 $molecule^{-1}$ s^{-1} at 298 K, which is also in excellent agreement

TABLE 3: Rate Constant for OH + *n*-Decane at 240−340 K

T (K)	reference compound[a]	slope[b]	$k_3 \times 10^{11}$ (cm^3 $molecule^{-1}$ s^{-1})	P_{total} (Torr)	technique	reference
240	1,4-dioxane	1.049 ± 0.060 (25)	1.21 ± 0.11	1.0−1.1	RR/DF/MS	this work
260	1,4-dioxane	1.075 ± 0.087 (23)	1.21 ± 0.13	1.0−1.1	RR/DF/MS	this work
277	1,4-dioxane	1.103 ± 0.060 (53)	1.22 ± 0.10	1.0−1.1	RR/DF/MS	this work
298	1,4-dioxane	1.183 ± 0.065 (65)	1.29 ± 0.11	1.0−1.1	RR/DF/MS	this work
320	1,4-dioxane	1.330 ± 0.061 (41)	1.42 ± 0.11	1.0−1.1	RR/DF/MS	this work
340	1,4-dioxane	1.374 ± 0.071 (40)	1.44 ± 0.12	1.0−1.1	RR/DF/MS	this work
298	diethyl ether	1.072 ± 0.038 (90)	1.39 ± 0.08	1.0−1.1	RR/DF/MS	this work
298	1,4-dioxane & *n*-octane	1.204 ± 0.050 1.603 ± 0.052	1.38 ± 0.08	1.0−1.1	RR/DF/MS	[27]
299 ± 2	*n*-hexane	n/a	1.14 ± 0.06	735	RR/DP/GC	[23]
312	*n*-heptane	n/a	1.17 ± 0.04	757.56	RR/DP/GC	[22]
300	*n*-octane	n/a	1.15 ± 0.02	800	RR	[34]
296 ± 2	*n*-octane	1.44 ± 0.04	1.25 ± 0.04	740	RR/GC-FID	[19]
298	n/a	n/a	1.22	n/a	transition-state theory	[37]

[a] The rate constant of the hydroxyl radical reaction with 1,4-dioxane and diethyl ether were calculated from Arrhenious equations previously published.[32,33] [b] The error bar was taken as 2σ. The number in parentheses represents the number of data points collected at corresponding temperature. [c] RF: Relative rate; DF: diffraction flow; DP: Direct Photolysis; MS: Mass Spectrometer; FP: Flash photolysis; GC: Gas Chromatography; FID: Flame Ionization Detection; TST: transition state theory.

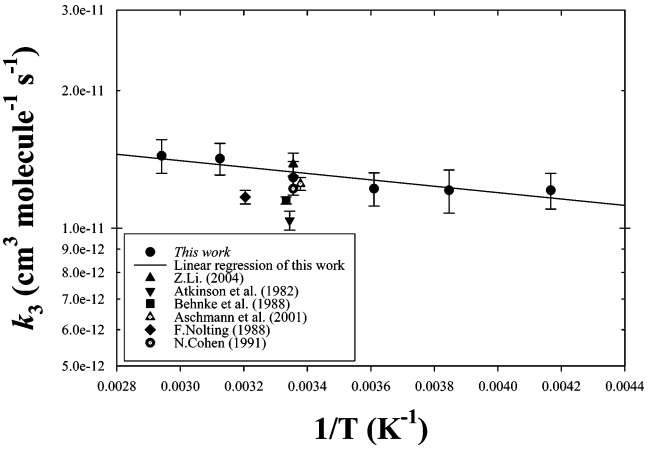

Figure 7. Arrhenius plot for the reaction of *n*-decane + OH at 240−340 K.

with the value of $k_3 = (1.38 \pm 0.08) \times 10^{-11}$ cm^3 $molecule^{-1}$ s^{-1} determined using 1,4-dioxane and *n*-octane as reference compounds.[27] Table 3 shows the rate constant for the reaction of OH + *n*-decane at 240−340 K along with available k_3 values in the literature. Fitting our experimental data into the Arrhenius equation (Figure 7) yields $k_3 = (2.26 \pm 0.28) \times 10^{-11} \times \exp[-(160 \pm 36)/T]$ cm^3 $molecule^{-1}$ s^{-1} at 240−340 K. We also believe that this is the first report of the temperature dependence investigation of the rate constant for the reaction of OH with *n*-decane.

On the basis of kinetic results, it is clear that the rate constant of OH + C_8−C_{10} *n*-alkane increases both with temperature and with the number of carbons of the hydrocarbon molecule. This observation indicates that reactions 1−3 proceed with hydrogen abstraction from the alkanes, and the increase of the carbon number will increase the number of $-CH_2-$ groups and hence the number of hydrogen atoms available for the abstraction, giving rise to a larger rate constant.

D. Atmospheric Lifetime of *n*-Octane, *n*-Nonane, and *n*-Decane. While there are several oxidants that can initiate the oxidation of C_8−C_{10} *n*-alkane in the troposphere, hydroxyl radicals are primarily responsible for the removal of these alkanes in the atmosphere.[38] The atmospheric lifetime of these molecules are then estimated using the following equation:

$$\tau_{alkane} \approx \frac{1}{k_{alkane+OH}[OH]} \qquad \text{(II)}$$

TABLE 4: Calculated Atmospheric Lifetimes of *n*-Octane, *n*-Nonane, and *n*-Decane

compound	*k* (277 K) (cm^3 $molecule^{-1}$ s^{-1})	τ_{alkane} (hours)
n-octane	7.91×10^{-12}	44
n-nonane	9.69×10^{-12}	36
n-decane	12.2×10^{-12}	28

where τ_{alkane} is the atmospheric lifetime of the alkane because of reactions with the OH radicals, $k_{alkane+OH}$ is the rate constant of reaction of alkane with OH radicals at typical tropospheric temperature of 277 K, and [OH] is the atmospheric concentration of the hydroxyl radicals. The average tropospheric hydroxyl concentration has previously been found to be $(8.1 \pm 0.9) \times 10^5$ molecules cm^{-3}.[39] Using the $k_{alkane+OH}$ (277 K) values determined in the present work, the atmospheric lifetime for *n*-octane, *n*-nonane, and *n*-decane are estimated to be 44, 36, and 28 h, respectively. The estimated lifetime of these alkanes is given in Table 4.

4. Summary

The kinetics of the reactions of OH with *n*-octane, *n*-nonane, and *n*-decane has been investigated in the temperature range of 240−340 K using the relative rate/discharge flow/mass spectrometry (RR/DF/MS) method. At 298 K, the rate constants for these reactions were determined to be $k_1 = (8.48 \pm 0.61) \times 10^{-12}$, $k_2 = (1.13 \pm 0.12) \times 10^{-11}$, and $k_3 = (1.29 \pm 0.11) \times 10^{-11}$ cm^3 $molecule^{-1}$ s^{-1}, respectively, which are in good agreement with literature values. The Arrhenius expression for these reactions were determined to be $k_1 = (2.27 \pm 0.21) \times 10^{-11} \exp[(-296 \pm 27)/T]$, $k_2 = (4.35 \pm 0.49) \times 10^{-11} \times \exp[(-411 \pm 32)/T]$, and $k_3 = (2.26 \pm 0.28) \times 10^{-11} \times \exp[(-160 \pm 36)/T]$ cm^3 $molecule^{-1}$ s^{-1} at 240−340 K, respectively, indicating a positive temperature dependence of rate constant for these reactions. Assuming that the C_8−C_{10} *n*-alkanes are removed from the troposphere mainly by OH attack, the atmospheric lifetime for *n*-octane, *n*-nonane, and *n*-decane are predicted to be 44, 36, and 28 hours, respectively.

Acknowledgment. This work was supported in part by the National Science Foundation (NSF CHE 0354159 and NSF ATM-0533574), the CSU Special Fund for Research, Scholarship, and Creative Activity Minigrant, and the Untenured Faculty Support Grants of CSUF.

References and Notes

(1) Grosjean, E.; Grosjean, D.; Rasmussen, R. A. *Environ. Sci. Technol.* **1998**, *32*, 2061.

(2) Chock, D. P.; Winkler, S. L.; Chang, T. Y.; Rudy, S. J.; Shen, Z. K. *Atmos. Environ.* **1994**, *28*, 2777.

(3) Agosta, A.; Cernansky, N. P.; Miller, D. L.; Faravelli, T.; Ranzi, E. *Exp. Therm. Fluid Sci.* **2004**, *28*, 701.

(4) Seinfeld, J. H.; Pandis, S. N. *Atmospheric Chemistry and Physics*; John Wiley and Sons, Inc.: New York, 1998.

(5) Zielinska, B.; Sagebiel, J. C.; Harshfield, G.; Gertler, A. W.; Pierson, W. R. *Atmos. Environ.* **1996**, *30*, 2269.

(6) Schauer, J. J.; Kleeman, M. J.; Cass, G. R.; Simoneit, B. R. T. *Environ. Sci. Technol.* **2002**, *36*, 1169.

(7) Schauer, J. J.; Kleeman, M. J.; Cass, G. R.; Simoneit, B. R. T. *Environ. Sci. Technol.* **1999**, *33*, 1566. Grosjean, E.; Grosjean, D.; Rasmussen, R. A. *Environ. Sci. Technol.* **1998**, *32*, 2061. Grosjean, E.; Rasmussen, R. A.; Grosjean, D. *Atmos. Environ.* **1998**, *32*, 3371.

(8) Barletta, B.; Meinardi, S.; Simpson, I. J.; Khwaja, H. J.; Blake, D. R.; Rowland, F. S. *Atmos. Environ.* **2002**, *36*, 3429.

(9) Grosjean, E.; Rasmussen, R. A.; Grosjean, D. *Atmos. Environ.* **1998**, *32*, 3371.

(10) California Environmental Protection Agency Web site. http://www.arb.ca.gov/regact/conspro/aerocoat/att1.doc/December 2005.

(11) Carter, W. P. L. J. *Air Waste Manage. Assoc.* **1994**, *44*, 881.

(12) Lim, Y. B.; Ziemann, P. J. *Environ. Sci. Technol.* **2005**, *39*, 9229.

(13) Finlayson-Pitts, B. J.; Pitts, J. N., Jr. *Chemistry of the upper and lower atmosphere*; Academic Press: San Diego, 2000.

(14) Darnall, K. R.; Carter, W. P. L.; Winter, A. M.; Lloyd, A. C.; Pitts, J. N., Jr. *J. Phys. Chem.* **1976**, *80*, 1948.

(15) Arey, J.; Aschmann, S. M.; Kwok, E. S. C.; Atkinson, R. *J. Phys. Chem. A* **2001**, *105*, 1020.

(16) Koffend, J. B.; Cohen, N. *Int. J. Chem. Kinet.* **1996**, *28*, 79.

(17) Donahue, N. M.; Anderson, J. G. *J. Phys. Chem. A* **1998**, *102*, 3121.

(18) Greiner, N. R. *J. Chem. Phys.* **1970**, *53*, 1070.

(19) Aschmann, S. M.; Arey, J.; Atkinson, R. *J. Phys. Chem. A* **2001**, *105*, 7598.

(20) Atkinson, R.; Aschmann, S. M.; Winer, A. M.; Pitts, J. N., Jr. *Int. J. Chem. Kinet.* **1982**, *14*, 507.

(21) Atkinson, R. *Chem. Rev.* **1985**, *85*, 69.

(22) Nolting, F.; Behnke, W.; Zetzsch, C. *J. Atmos. Chem.* **1988**, *6*, 47.

(23) Atkinson, R.; Aschmann, S. M.; Winer, A. M.; Pitts, J. N., Jr. *Int. J. Chem. Kinet.* **1982**, *14*, 781.

(24) Coeur, C.; Jacob, V.; Foster, P.; Baussand, P. *Int. J. Chem. Kinet.* **1998**, *30*, 497.

(25) Ferrari, C.; Roche, A.; Jacob, V.; Foster, P.; Baussand, P. *Int. J. Chem. Kinet.* **1996**, *28*, 609.

(26) Wilson, E. W., Jr.; Hamilton, W. A.; Kennington, H. R.; Evans, B., III; Scott, N. W.; DeMore, W. B. *J. Phys. Chem. A* **2006**, *110*, 3593.

(27) Li, Z. *Chem. Phys. Lett.* **2004**, *383*, 592.

(28) Li, Z.; Pirasteh, A. *Int. J. Chem. Kinet.* **2006**, *38*, 386.

(29) Li, Z.; Nguyen, P.; de Leon, M. F.; Wang, J. H.; Han, K.; He, G. Z. *J. Phys. Chem. A* **2006**, *110*, 2698.

(30) Sander, S. P.; Friedl, R. R.; Golden, D. M.; Kurylo, M. J.; Huie, R. E.; Orkin, V. L.; Moortgat, G. K.; Ravishankara, A. R.; Kolb, C. E.; Molina, M. J.; Finlayson-Pitts, B. J. *Chemical Kinetics and Photochemical Data for Use in Stratospheric Modeling*; JPL Publication 02-25; JPL: Pasadena, CA, 2003.

(31) Steinfeld, J. I.; Francisco, J. S.; Hase, W. L. *Chemical Kinetics and Dynamics*, 2nd ed.; Prentice-Hall Inc.: Upper Saddle River, NJ, 1998.

(32) Dagaut, P.; Liu, R.; Wallington, J.; Kurylo, M. J. *J. Phys. Chem.* **1990**, *94*, 1881.

(33) Bennett, P. J.; Kerr J. A. *J. Atmos. Chem.* **1990**, *10*, 29.

(34) Behnke, W.; Holländer, W.; Koch, W.; Nolting, F.; Zetch, C. *Atmos. Environ.* **1988**, *22*, 1113.

(35) Kramp, F.; Paulson, S. E. *J. Phys. Chem. A* **1998**, *102*, 2685.

(36) Colomb, A.; Jacob, V.; Kaluzny, P.; Baussand, P. *Int. J. Chem. Kinet.* **2004**, *36*, 367.

(37) Cohen, N. *Int. J. Chem. Kinet.* **1991**, *23*, 397.

(38) Li, Z.; Jeong, G.; Hansen, J. C.; Good, D. A.; Francisco, J. S. *Chem. Phys. Lett.* **2000**, *320*, 70.

(39) Prinn, P.; Cunnold, D.; Simmonds, P.; Alyea, F.; Bold, R.; Crawford, A.; Fraser, P.; Gutzler, D.; Hartley, D.; Rosen, R.; Rasmussen, R. *J. Geophys. Res.* **1992**, *97*, 2445.